

Covalent Functionalized Carbon Nanotube with Ionic Liquid and Its Application for Human Immunoglobulin G Immunosensor

Guangyu Shen*, Youming Shen

Hunan Province Cooperative Innovation Center for The Construction & Development of Dongting Lake Ecological Economic Zone, College of Chemistry and Material Engineering, Hunan University of Arts and Science, Changde, 415000, PR China

*E-mail: sgyrab@163.com

Received: 16 April 2019 / Accepted: 31 May 2019 / Published: 30 June 2019

In this work, ionic liquid functionalized carbon nanotube was simply prepared via covalent bond between aldehyde-terminated ionic liquid and amino-terminated carbon nanotube. The combination overcame the shortages and shared the advantages of both ionic liquids and carbon nanotube. On the one hand, ionic liquid was prevented to leach out from electrode surface to electrolyte solution, which resulting a stable sensing interface. In the meantime, the degree of curling of CNT was decreased. On the other hand, this novel hybrid nanomaterial can further improve the conductivity of film modified on the electrode surface. The prepared immunosensor was used to detect human IgG in a linear range of 0.1-15 ng mL⁻¹. The detection limit was 0.02 ng mL⁻¹ ($S/N=3$). The electrochemical immunosensor with film fabricated with the hybrid nanomaterial had satisfactory reproducibility, high sensitivity, acceptable specificity and good stability.

Keywords: Ionic liquid; Covalent functionalized carbon nanotube; Chitosan; Electrochemical immunosensor

1. INTRODUCTION

Ionic liquids (IL) possess several useful features such as biocompatibility, high ionic conductivity, electrochemical stability and biocompatibility. They have been widely applied in the fabrication of electrochemical immunosensors by being mixed with conventional matrixes such as biopolymers, cellulose, nanoparticles, and graphene to form composite materials [1-4]. Due to the introduction of IL, the composite materials not only provided a good microenvironment for immobilizing proteins, but also improved the conductivity of the modifying films [5,6].

Carbon nanotubes (CNT) as molecular wires have attracted considerable interests due to their good electrical conductivity, high chemical stability and modifiable sidewalls. For example, CNT have been used as additive to improve direct electron transport of sensing interface [7-10]. However, due to the vander Waals interaction and π - π stacking, CNT were easy to entangle with each other and formed agglomerates [11,12], which hindered the dispersing of CNT in substrate. It was reported that IL were mixed with CNT to forming a thermally stable gel, in which CNT exist as untangled three dimensional network bundles due to cation- π interactions of the IL and CNT surfaces [13,14]. However, IL can leach out from the electrode surface to electrolyte solution due to the weak electrostatic interaction, resulting in the instability of electrochemical signals.

To date, researches of how to attach ionic liquid to the surface of CNT through covalent bond have not been reported. A covalent binding between the amine groups and the aldehyde groups should easily occur. In this work, amine-containing CNT was functionalized with aldehyde-terminated ionic liquid, leading to the formation of a novel hybrid nanomaterial (CNT-IL). Chitosan (Chit) has many useful features including biocompatibility, film forming ability, nontoxicity, and high mechanical strength. It has been widely applied in the fabrication of biosensor [15,16]. In the present study, the mixture of CNT-IL and Chit was modified on the Au electrode surface to fabricate a biosensing platform. The immunosensor based on CNT-IL/Chit was advantageous because of the following: (1) keeping inherent properties of CNT and IL; (2) better conductivity property; (3) avoiding the tangle of CNT and the leach out of the IL from electrode surface to electrolyte solution; (4) the sensitivity and stability can be improved. Using the novel hybrid nanomaterial, we fabricated an immunosensor for the determination of human immunoglobulin G.

2. EXPERIMENTAL

2.1. Reagents and apparatus

We obtained bovine serum albumin (BSA), rabbit anti-human IgG antibody (Ab), and human immunoglobulin G (IgG) from Beijing Dingguo Biotechnology Company (Beijing, China). Other reagents were come from Sigma-Aldrich (St. Louis, MO). Aldehyde-terminated ionic liquid (IL-CHO) was synthesized by our group. Amine-terminated CNT (CNT-NH₂) was purchased from Nanjing Xianfeng nanomaterial Technology Ltd. We prepared 0.1 M phosphate buffer solution (PBS, pH 7.0) using Na₂HPO₄ and KH₂PO₄, which was used for the supporting electrolyte and preparing the antibody, antigen, and BSA solution. By dissolving 10 mg chitosan (Chit) in 2.0 mL of 0.1 mol/L acetic acid, A 5 mg/mL Chit solution was prepared. The film-forming solution was prepared by dissolving 1 mg ionic liquid-functionalized CNT (CNT-IL) in 1 mL 0.1 mol/L Chit solution.

2.2. Preparation ionic liquid-functionalized CNT (CNT-IL)

IL-CHO was synthesized as reported work by our group [17]. CNT-IL composite was synthesized by a covalent binding between the amine groups of CNT-NH₂ and the aldehyde groups of

IL-CHO (Fig. 1). Typically, 2.0 mg of CNT-NH₂, 20.0 mg of IL-CHO were mixed with 10.0 ml of ultrapure water. After the mixture was ultrasonicated for 30 min followed by strongly stirring for 2 h, the resulting homogeneous mixture was subsequently centrifuged at 12000 rpm for 10 min and washed three times with ultrapure water. The CNT-IL hybrid nanomaterial was obtained. Then the CNT-IL product was redispersed into Chit solution (Chit/CNT-IL). The concentration of CNT-IL was 1.0 mg mL⁻¹.

2.3. Fabrication of immunosensor

Prior to modifying the gold electrode (Au, 3 mm in diameter), it was polished repeatedly with 0.3 and 0.05 μm alumina slurries. Then the electrode was cleaned with hot piranha solution (a 3:1 mixture of H₂SO₄ and H₂O₂, v/v) several times followed by washing with water. Chit/CNT-IL-modified electrode (Chit/CNT-IL/Au) was obtained by dropping 10 μL of Chit/CNT-IL solution on the surface of cleaned Au electrode, followed by drying in the air. Then, 10 μL of 5% glutaraldehyde (GA) aqueous solution was added on Chit/CNT-IL film-modified electrode (GA/Chit/CNT-IL/Au). After 60 min, the electrode was thoroughly washed with water, followed by drop-casting 10 μL of 75 μg mL⁻¹ antibody solution on the electrode to be incubated for 40 min at 37 °C (Ab/GA/Chit/CNT-IL/Au). In order to remove unconjugated antibodies with glutaraldehyde, the obtained electrode was washed with PBS (pH 7.0). After that, 10 μL BSA (2.0 wt%) was dropped on antibody-modified electrode to be incubated for 40 min at 37 °C for the purpose of eliminating nonspecific reaction (BSA/Ab/GA/Chit/CNT-IL/Au). After the electrode modified with BSA was washed with PBS (pH 7.0), 10 μL of antigen solution with different concentration was added on the electrode, followed by incubation for 40 min at 37 °C (IgG/BSA/Ab/GA/Chit/CNT-IL/Au). In addition, we prepared the electrode modified with Chit and CNT-NH₂ (Chit/CNT-NH₂/Au).

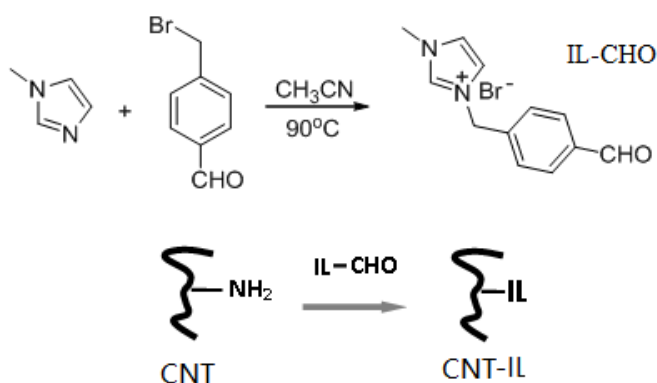


Figure 1. Illustration of the preparation of IL-CHO and CNT-IL.

2.4. Electrochemical Measurements

DPV measurements were carried out in 10 mM K₃[Fe(CN)₆]/K₄[Fe(CN)₆] under the following: the potential range was from 0.2 to 0.8 V, pulse amplitude was 0.05 V, pulse width was 0.05 s, and

sample width was 0.02 s. CV measurements were carried out in 10 mM $K_3[Fe(CN)_6]/K_4[Fe(CN)_6]$. The scan rate was 100 mV s^{-1} and the potential range was from -0.2 to 0.6 V .

3. RESULTS AND DISCUSSION

3.1. Characterization of IL-functionalized CNT (CNT-IL)

The CNT-IL was characterized by UV-vis spectroscopy. The results were showed in Fig. 2A. The UV-vis spectrogram of IL-CHO has two absorption peaks at 259 and 306 nm. No absorption peaks of UV-vis spectrogram of CNT-NH₂ was observed (Fig. 2A, b). The absorption peaks of UV-vis spectrogram of CNT-IL nanocomposite at 265 and 310 nm (Fig. 2A, c), resulting in a red shift, which demonstrated IL-CHO was successfully bound to CNT-NH₂. The surface structure and shape of the CNT-NH₂ (Fig. 2B) and CNT-IL nanocomposite (Fig. 2C) was examined with scanning electron microscopy. As can be seen from Fig. 2B, CNT-NH₂ looked like noodles and heavily entangled with each other. After CNT-NH₂ was functionalized with IL-CHO, the degree of curling was greatly reduced (Fig. 2C). It could be ascribed to cation- π interactions of the IL-CHO and CNT-NH₂ surfaces. IR-spectra of CNT-IL was also measured. Fig. 2D showed CNT-IL has an obvious C=N peak at 1630 cm^{-1} . This result demonstrated that the CNT-IL had been synthesized successfully.

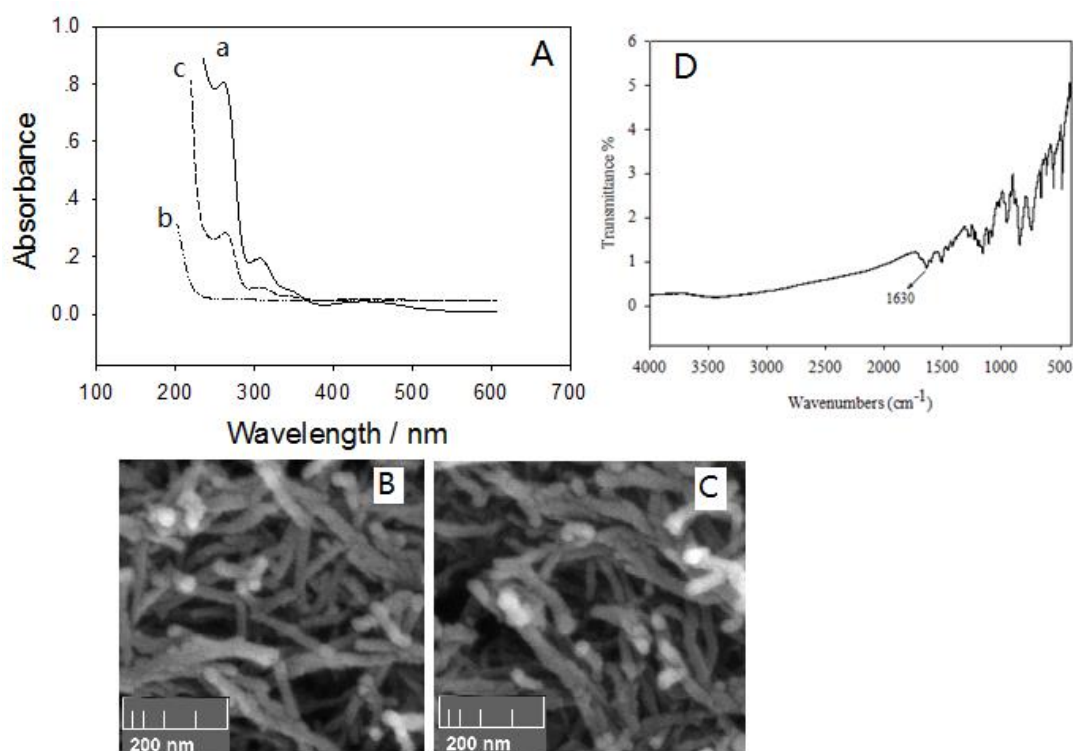


Figure 2. (A) UV-vis spectra of IL-CHO (a), CNT-NH₂ (b) and CNT-IL (c). (B) The morphology of scanning electron microscopy of CNT-NH₂. (C) The morphology of scanning electron microscopy of the CNT-IL nanocomposite. (D) FTIR spectra of CNT-IL.

3.2. Cyclic voltammetric characterization of the electrode modified

When the electrode is modified step by step, the changes of the electrochemical properties of the electrode surface will take place [18]. As can be seen from Fig. 3, the CV spectrum of bare electrode was a well-defined redox wave (a). After the Chit/CNT-NH₂ film was modified on the bare electrode, the peak current of CV spectrum corresponding to Chit/CNT-NH₂/Au electrode increased (b). More importantly, when the electrode was modified with Chit/CNT-IL composite film, the peak current of CV spectrum was further increased (c). It is because CNT-IL hybrids were effectively improved electrical properties of the electrode surface [19]. When GA aqueous solution was added on Chit/CNT-IL film-modified electrode, the peak current of CV spectrum was decreased (d). After the electrode modified was incubated with antibody solution, the peak current of CV spectrum continued to decline (e), indicating that antibodies were successfully immobilized on the electrode. In the following step, BSA solution was added onto antibody-modified electrode for reducing the nonspecific binding, the peak current of CV spectrum decreased (f). Finally, the electrode modified with BSA was incubated with antigen, the peak current of CV spectrum further decreased (g) due to the antibody-antigen immunocomplex blocked the tunnel for mass and electron transfer [20].

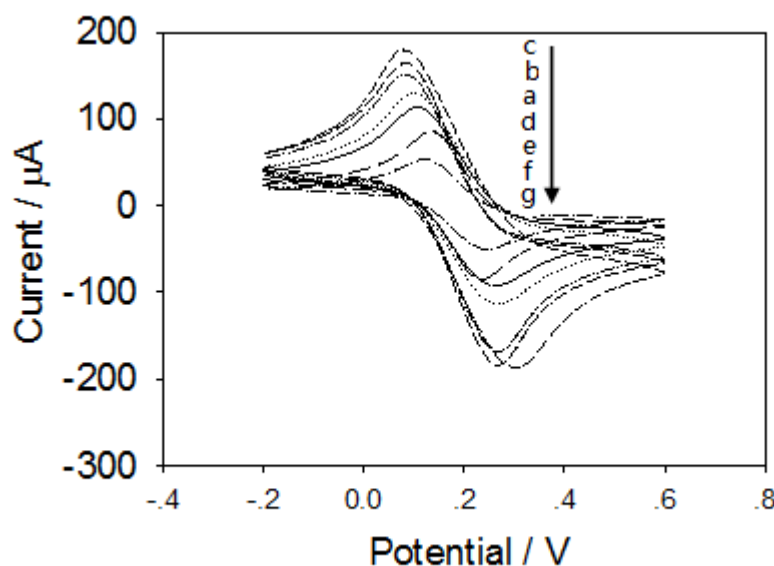


Figure 3. CV profiles of the different modified electrodes: bare Au electrode (a), Chit/CNT-NH₂/Au (b), Chit/CNT-IL/Au (c), GA/Chit/CNT-IL/Au (d), Ab/GA/Chit/CNT-IL/Au (e), BSA/Ab/GA/Chit/CNT-IL/Au (f), IgG/BSA/Ab/GA/Chit/CNT-IL/Au (g). The concentration of IgG is 10 ng mL⁻¹.

3.3. Stability of different films

It is reported that the sensing interface based on IL-functionalized graphene sheets possessed good stability [21]. Here, we compared the stability of three different film made of Chit/CNT-NH₂, Chit/IL-CHO and Chit/CNT-IL, respectively. When those film was modified on the electrode surface, CV signals were measured continuously 4 times. Fig. 4A showed that the CV profiles of the electrode

modified with Chit/CNT-NH₂ film overlapped and therefore no significant change of peak current was observed. Thus, the Chit/CNT-NH₂ film was stable. However, the peak current of the electrode modified with Chit/IL-CHO film decreased from 145 to 120 μA after scan the same cycles ($n=4$) (Fig. 4B), indicating the Chit/IL-CHO film was unstable probably due to the leach out of the IL-CHO from electrode surface to electrolyte solution. Fortunately, when IL-CHO was bound to CNT-NH₂ via covalent interaction, the peak current of the electrode modified with Chit/CNT-IL film was increased and no obvious changes after 4 times scan (Fig. 4C), demonstrating that the combine of CNT-NH₂ with IL-CHO not only prevented the leach of IL-CHO, but also improved the conductivity of film.

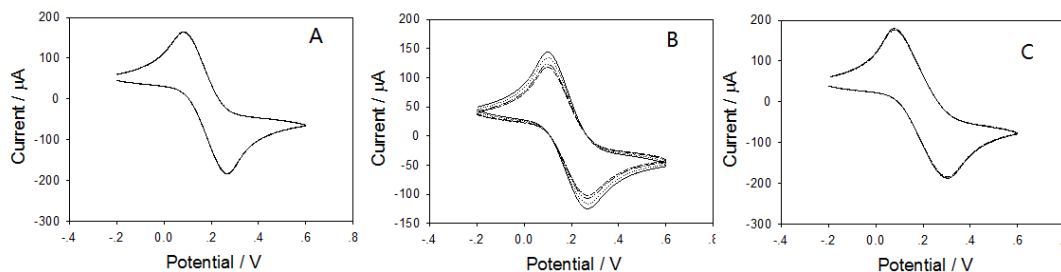


Figure 4. The stability of different films: (A) Chit/CNT-NH₂ film, (B) Chit/IL-CHO film, (C) Chit/CNT-IL film. The number of scanning was 4.

3.4. Investigation of experimental conditions

Here, GA was used as a “bridge” reagent, which linked Chit and antibody. The interaction time of Chit with GA was studied by DPV in the time region from 20 to 80 min at room temperature. Fig. 5A displayed short reaction time gave higher response because lesser antigen was captured by antibody. 60 min later, a platform appeared. Thus, we adopted 60 min for further experiments.

The concentration of antibody was investigated in the range of 25 to 100 $\mu\text{g mL}^{-1}$ at room temperature. Antibody solution with different concentration was incubated with the same IgG target with concentration of 10 ng mL^{-1} . Fig. 5B showed that the antibody concentration of 75 $\mu\text{g mL}^{-1}$ was an optimal selection.

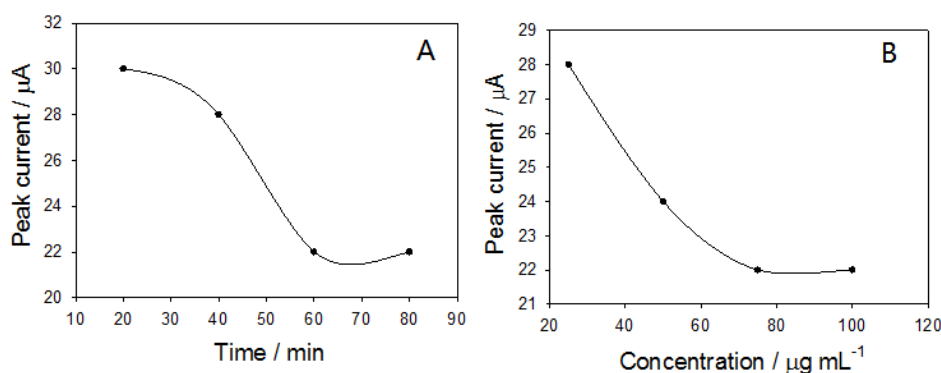


Figure 5. Effect of reaction time of Chit with GA (A), antibody concentration (B) on the peak current of immunosensor. The concentration of IgG is 10 ng mL^{-1} .

3.5. The determination of IgG

When the antibody-antigen immunocomplex formed on the electrode, it would hinder electron transfer, and thus the peak current of DPV increased as decreasing concentration of IgG (Fig. 6A). Fig. 6B indicated a linear calibration was obtained in the range of 0.1- 15 ng mL⁻¹. The detection limit was 0.02 ng mL⁻¹ (S/N = 3).

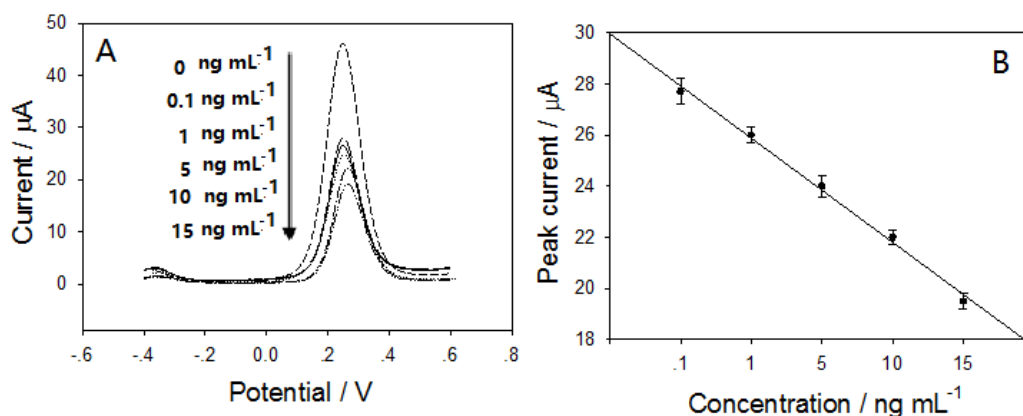


Figure 6. (A) DPV responses of the immunosensor to different concentrations of IgG. (B) Calibration curve of the immunosensor to different concentrations of IgG. Error bars represent standard deviation, n=3.

We compared the analytical characteristics including the detection limit and linear range of this IgG immunosensor with that of other IgG immunosensors. As shown in Table 1, although the fabricated immunosensor had a narrower linear range, it exhibited a lower detection limit. The high sensitivity can be attributed to several factors. Firstly, the hybrid nanomaterial of CNT-NH₂ and IL-CHO can improve the conductivity of sensing interface. Secondly, due to covalent bond between aldehyde-terminated ionic liquid and amino-terminated carbon nanotube, the ionic liquid was prevented to leach out from electrode surface to electrolyte solution, which helped to capture the IgG onto the electrode surface through immune reaction and resulted in strong electrochemical signal.

Table 1. Comparison of the proposed immunosensor and other sensors.

Detection methods	Linear range (ng.mL ⁻¹)	detection limit (ng.mL ⁻¹)	References
Amperometry	0.82–90	0.25	[22]
Amperometry	2–100	1.70	[23]
DPV	0.5–45	0.3	[24]
EIS	0.5–125	0.02	[25]
DPV	2-300	0.8	[26]
DPV	30-1000	25	[27]
DPV	0.1–10	0.03	[6]
DPV	0.1–15	0.02	This work

3.6. Reproducibility, specificity and stability of the immunosensor

We investigated the reproducibility of proposed immunosensor by inter- and intra-assay at 5 ng mL^{-1} IgG. The coefficients of variation were 8.5% for inter-assay and 5.3% for intra-assay, suggesting that the developed immunosensor possessed a satisfactory reproducibility.

Using some interfering species including carcinoembryonic antigen (CEA), BSA and α -fetoprotein (AFP), we investigated the specificity of the proposed immunosensor. The DPV signals were measured and those results were shown in Fig. 7. As can be seen from Fig. 7, the peak current of DPV toward higher concentration (100 ng mL^{-1}) of interfering substances were close to the response toward blank solution. However, the peak current of DPV toward of IgG (5 ng mL^{-1}) was much lower than that of interfering substances, indicating the specificity of the prepared immunosensor had a good specificity.

In order to estimate the stability of immunosensor, the initial DPV was measured. After one week, the DPV current response decreased 4.1%. After four weeks, the DPV current response decreased 7.7%. The results demonstrated the designed immunosensor has satisfied stability.

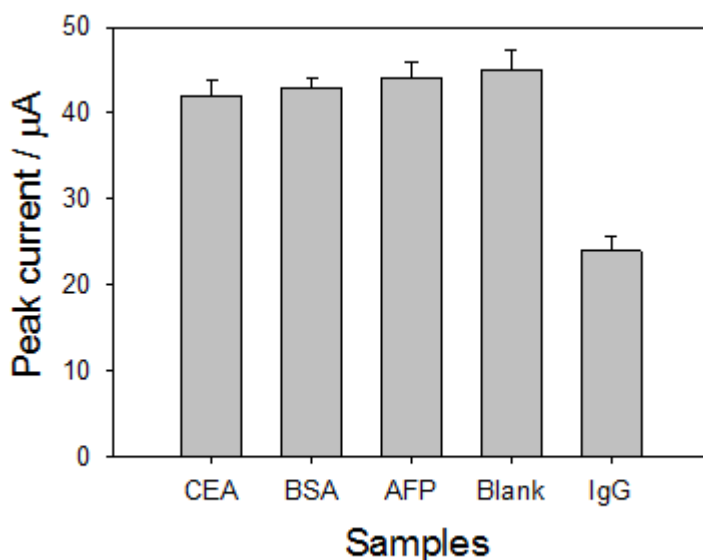


Figure 7. Specificity of the immunosensor. The concentration of nonspecific materials is 100 ng mL^{-1} and the concentration of IgG is 5 ng mL^{-1} , Error bars represent standard deviation, $n=3$.

3.7. Detect IgG in real samples

For investigating the practical application in clinical detection, three real human serum samples supplied by local hospital were analyzed using the developed immunosensor. The analytical results were compared with those resulted from ELISA method. By comparing experimental results (Table 2), there were no significant differences between two methods, indicating a good correlation between ELISA and this proposed method. The proposed immunosensor was reliable for IgG detection.

Table 2. Serum sample analysis and the comparison with ELISA method (n=5).

Samples	ELISA (ng mL ⁻¹)	This method (ng mL ⁻¹)	Relative error (%)
1	4.33	4.58	5.5
2	12.50	11.75	-6.4
3	6.89	7.09	2.8

4. CONCLUSIONS

Here, CNT-NH₂ was functionalized with ionic liquid via covalent bond. The results from UV-vis spectrogram and IR-spectra of CNT-IL clearly indicate that the IL-CHO was coupled to the surface of the CNT-NH₂ successfully. Additionally, the combine of CNT-NH₂ with IL-CHO not only prevented the leach of IL-CHO, but also improved the conductivity of sensing film. The immunosensor for human IgG exhibited some good analytical performance such as satisfactory reproducibility, good specificity and acceptable stability. Furthermore, CNT-IL nanocomposite was an attractive modifying material in the fabrication of other electrochemical biosensors.

ACKNOWLEDGMENTS

This work was supported by Hunan Provincial Natural Science Foundation of China (2016JJ6105).

References

1. J.F. Fei, W.C. Dou, G.Y. Zhao, *Microchim. Acta*, 182 (2015) 2267.
2. N. Lin, X. Chen, Z.F. Ma, *Biosens. Bioelectron.*, 48 (2013) 33.
3. X.L. Wang, J.C. Hao, *Sci. Bull.*, 61(2016) 1281.
4. C.C Liu, Q. Deng, G.Z. Fang, M. Dang, S. Wang, *Anal. Biochem.*, 530 (2017) 50.
5. Y. Wei, X. Li, X. Sun, H. Ma, Y. Zhang, Q. Wei, *Biosens. Bioelectron.*, 94 (2017) 141.
6. S. Dong, M. Tong, D. Zhang, T. Huang, *Sens. Actuators B*, 251 (2017) 650.
7. P.P. Samadi, H. Ghanbari, R. Saber, Y. Omid, *Biosens. Bioelectron.*, 30 (2018) 68.
8. M.A. Hussein, K.A. Alamry, F.M.A. Shehry, A.M. Asiri, *Talanta*, 150 (2016) 71.
9. P. Gulati, P. Kaur, M.V. Rajam, T. Srivastava, S.S. Islam, *Anal. Biochem.*, 557 (2018) 111.
10. M.P. Costa, I.A.M. Frías, C.A.S. Andrade, M.D.L. Oliveira, *Microchim. Acta*, 184 (2017) 3205.
11. M.J. Shiddiky, A.A. Torriero, *Biosens. Bioelectron.*, 26 (2011) 1775.
12. S. Singal, A.K. Srivastava, B.J. Rajesh, *Microchim. Acta*, 183(2016) 1375.
13. X. Zhang, W. Dou, X. Zhan, G. Zhao, *Electrochim. Acta*, 61 (2012) 73.
14. A.H. Ali, A.A. Mohammed, H. Maan, J. Ibrahim, A.H. Mohd, *Electrochim. Acta*, 193 (2016) 321.
15. E.B. Aydın, M. Aydın, M.K. Sezginürk, *Biosens. Bioelectron.*, 121 (2018) 80.
16. R. Devi, S. Gogoi, S. Barua, H.S. Dutta, R. Khan, *Food Chem.*, 276 (2019) 350.
17. Y. Shen, G. Shen, Y. Zhang, C. Zhang, H. Li, *Talanta*, 175 (2017) 347.
18. L. Liu, Z. Zheng, C. Gu, X. Wang, *Compos. Sci. Technol.*, 70 (2010) 1697.
19. A.K. Ghamsari, S. Wicker, E. Woldesenbet, *Compos. Part B: Eng.*, 67 (2014) 1.
20. S. Yu, X. Cao, M. Yu, *Microchem. J.*, 103 (2012) 125.
21. C. Shan, H. Yang, D. Han, Q. Zhang, A. Ivaska, L. Niu, *Biosens. Bioelectron.*, 25 (2010) 1504.

22. L. Zhang, Y. Liu, T. Chen, *Int. J. Biol. Macromol.*, 43 (2008) 165.
23. C. Thunkhamrak, P. Reanpang, K. Ounnunkad, J. Jakmunee, *Talanta*, 171 (2017) 53.
24. X. Zhang, G. Shen, S. Sun, Y. Shen, C. Zhang, A. Xiao, *Sens. Actuators B*, 200 (2014) 304.
25. M.A. Tabrizi, M. Shamsipur, A. Mostafaie, *Mater. Sci. Eng. C*, 59 (2016) 965.
26. S. Dong, M. Li, W. Wei, D. Liu, T. Huang, *J. Solid State Electrochem.*, 21 (2017) 793.
27. Z. Hajar, G. Hedayatollah, E. Khadijeh, Z. Majid, *Anal Biochem.*, 421 (2012) 446.

© 2019 The Authors. Published by ESG (www.electrochemsci.org). This article is an open access article distributed under the terms and conditions of the Creative Commons Attribution license (<http://creativecommons.org/licenses/by/4.0/>).